

χ_c Production in Hadronic Z Decays

The L3 Collaboration

Abstract

We report on inclusive χ_c production in Z decays reconstructed via the decay mode $\chi_c \rightarrow J + \gamma$. This analysis is based on 1.1 million hadronic Z events. Interpreting the observed signal as χ_{c1} , we obtain a branching ratio $\text{Br}(Z \rightarrow \chi_{c1} + X) = (7.5 \pm 2.9(\text{stat}) \pm 0.6(\text{sys})) \times 10^{-3}$. Assuming all events are produced in b decays we obtain $\text{Br}(b \rightarrow \chi_{c1} + X) = (2.4 \pm 0.9(\text{stat}) \pm 0.2(\text{sys})) \times 10^{-2}$. We also present an improved measurement of the branching ratio $\text{Br}(Z \rightarrow J + X) = (3.6 \pm 0.5(\text{stat}) \pm 0.4(\text{sys})) \times 10^{-3}$, obtained from dileptonic J decays.

(Submitted to Physics Letters B)

1 Introduction

The dominant mechanism for production of $c\bar{c}$ bound states in Z decays is expected to be

$$e^+e^- \rightarrow Z \rightarrow b\bar{b}; \quad b(\bar{b}) \rightarrow [c\bar{c}] + X. \quad (1)$$

The latter decay proceeds mainly through the internal W emission diagram [1–4] shown in figure 1, where the c and \bar{c} have to match in color. The production of $c\bar{c}$ bound states in B hadron decays offers a unique opportunity to study the interplay between weak and strong interactions. The production of χ_{c1} and η_c mesons in B decays is expected to arise through axial currents, whereas J and ψ' production proceeds via vector current coupling. If soft gluon exchange is neglected, the production of χ_{c0} and χ_{c2} states in b decays is forbidden [1, 2]. Recent results from ARGUS [5] on the inclusive branching ratio $\text{Br}(B \rightarrow \chi_{c1} + X)$ indicate a value higher than that predicted [1, 2].

In this paper, we report on an analysis performed on data collected with the L3 detector. This data corresponds to a sample of 1.1 million $e^+e^- \rightarrow \text{hadron}$ events, recorded in 1990, 1991 and 1992 at $\sqrt{s} \approx M_Z$. The decay of χ_c into $J + \gamma$ produces a photon of energy in the range 0 to 8 GeV in the laboratory frame. We describe the selection of J candidates and present an improved measurement of $\text{Br}(Z \rightarrow J + X)$. With these events we reconstruct χ_c mesons and measure the branching ratios $\text{Br}(Z \rightarrow \chi_{c1} + X)$ and $\text{Br}(b \rightarrow \chi_{c1} + X)$.

2 The L3 Detector

The L3 detector [6] consists of a central tracking chamber (TEC), a high resolution electromagnetic calorimeter composed of bismuth germanium oxide (BGO) crystals, a barrel of scintillation counters, a uranium and brass hadron calorimeter with proportional wire chamber readout and a high precision muon spectrometer. These detectors are located in a 12 m diameter magnet which provides a uniform field of 0.5 T along the beam direction. The material preceding the barrel part of the electromagnetic detector amounts to less than 10% of a radiation length. The energy resolution is 5% for photons and electrons at energies around 100 MeV and is less than 2% for energies above 1.5 GeV. The angular resolution of electromagnetic clusters is better than 0.5° for energies greater than 1 GeV. For the present analysis we use data collected in the following angular regions:

central tracking chamber:	$40^\circ \leq \theta \leq 140^\circ$,
electromagnetic calorimeter:	$42^\circ \leq \theta \leq 138^\circ$,
hadron calorimeter:	$5^\circ \leq \theta \leq 175^\circ$,
muon spectrometer:	$36^\circ \leq \theta \leq 144^\circ$,

where θ is defined with respect to the beam axis.

3 J Candidate Selection

The trigger requirements and the selection criteria for hadronic events containing electrons and muons have been described elsewhere [7]. Muons are identified and measured in the muon chamber system. We require that a muon track consists of track segments in at least two of the three layers of muon chambers, and that the muon track points to the interaction region. Electrons are identified using the BGO and hadron calorimeters, as well as the central tracking chamber. We require a cluster in the BGO that is consistent with the shape of an electromagnetic shower, as determined from test beam studies. To reject misidentified hadrons, we require that there be less than 3 GeV deposited in the hadron calorimeter in a cone of half opening angle 7° behind the electromagnetic cluster. The charge of the electron is determined using the TEC.

In the laboratory system, the decay $J \rightarrow \ell^+\ell^-$ typically results in one high and one low momentum lepton. We therefore select leptons with a momentum larger than 2 GeV, rather than the usual 3 or 4 GeV criterion used for other analyses [9]. We require the opening angle between two oppositely charged lepton candidates to be smaller than 90° .

Muon and electron pairs passing the above cuts can also arise from several different background sources. The dominant source is the semileptonic decay of a b hadron to a c hadron, followed by the semileptonic decay of the c hadron. Other sources are: a prompt lepton from a b or c hadron decay, accompanied by a misidentified hadron or lepton from K or π decay; a misidentified hadron with a lepton from K or π decay; and two misidentified hadrons. All these processes tend to give masses below that of the J. The background processes are simulated using 10^6 five flavor $Z \rightarrow q\bar{q}$ Monte Carlo events produced using the JETSET program [11]. The acceptance calculation was based on the fully simulated JETSET Monte Carlo b flavor events, imposing the decay chain $b \rightarrow J + X$ followed by $J \rightarrow \ell^+\ell^-$ for one of the b hadrons. The acceptance for $J \rightarrow \mu^+\mu^-$ is $\varepsilon_J = 0.25 \pm 0.017$ and is mainly determined by the angular coverage of the muon chambers and the absorption of low momentum muons in the calorimeter. The acceptance for $J \rightarrow e^+e^-$ is not only limited by the angular coverage of the BGO barrel electromagnetic calorimeter but also by the specific isolation requirements imposed by the electron selection criteria. The acceptance for $J \rightarrow e^+e^-$ is calculated to be $\varepsilon_J = 0.12 \pm 0.01$.

4 Determination of $\text{Br}(Z \rightarrow J + X)$

The measured invariant mass distributions of the $\mu^+\mu^-$ and e^+e^- pairs are shown in Figure 2. We fit the invariant mass distribution in the mass region $2.0 < M_{\ell^+\ell^-} < 4.0$ GeV with a Gaussian for the signal and an exponential function for the background. In the fit we constrain the standard deviation of the Gaussian width to the Monte Carlo value of 148 MeV for the $\mu^+\mu^-$ channel and 75 MeV for the e^+e^- channel. As can be seen from figure 2, the shape of the background is well reproduced by the simulation. We find 87 ± 13 $J \rightarrow \mu^+\mu^-$ events and 34 ± 7 $J \rightarrow e^+e^-$ events. The mass value of the J is found to be 3064 ± 23 MeV for $J \rightarrow \mu^+\mu^-$ and 3066 ± 16 MeV for $J \rightarrow e^+e^-$.

To determine the branching ratio $\text{Br}(Z \rightarrow J + X)$ we include our selection efficiency and measurements of the total and hadronic widths of the Z [12] and the measurement of $\text{Br}(J \rightarrow \mu^+\mu^-) = 0.0590 \pm 0.0015$ (*stat.*) ± 0.0019 (*sys.*) from the MARK-III experiment [14].

We find:

$$\text{Br}(Z \rightarrow J + X) = (3.9 \pm 0.6 \text{ (stat.)} \pm 0.4 \text{ (sys.)}) \times 10^{-3} \text{ from the } \mu^+ \mu^- \text{ channel.}$$

$$\text{Br}(Z \rightarrow J + X) = (3.1 \pm 0.7 \text{ (stat.)} \pm 0.4 \text{ (sys.)}) \times 10^{-3} \text{ from the } e^+ e^- \text{ channel.}$$

Contributions to the systematic error on $\text{Br}(Z \rightarrow J + X)$ are obtained by changing the fitting method and by varying the selection parameters by their errors. Combining the two measurements and taking into account common systematic errors, we obtain the branching ratio:

$$\text{Br}(Z \rightarrow J + X) = (3.6 \pm 0.5 \text{ (stat.)} \pm 0.4 \text{ (sys.)}) \times 10^{-3}.$$

Assuming that all J mesons are produced via b hadron decays, the branching ratio $\text{Br}(b \rightarrow J + X)$ can be deduced [8] using the L3 measurement of $\Gamma_{b\bar{b}}$ [9]. We find:

$$\text{Br}(b \rightarrow J + X) = (1.16 \pm 0.16 \text{ (stat.)} \pm 0.14 \text{ (sys.)}) \times 10^{-2}.$$

5 χ_c Candidate Selection

Inclusive χ_c meson production in Z decays is observed via $\chi_c \rightarrow J + \gamma$. In this study the J is reconstructed using only the $J \rightarrow \mu^+ \mu^-$ channel. We use the selected sample of J mesons with muon pairs having an invariant mass $2.8 < M_{\mu^+ \mu^-} < 3.4$ GeV.

A photon candidate is defined as an isolated energy cluster in the BGO having a shape consistent with an electromagnetic shower. We further require that there be no TEC tracks pointing to the cluster within 20 mrad in the r - ϕ plane and that the energy of the cluster be greater than 1 GeV. We further exclude all photons which result in a two-photon invariant mass compatible with that of a π^0 mass within 3σ of the BGO resolution (≈ 7 MeV) [10].

We require the opening angle between the J and the photon to be smaller than 50° in order to suppress the combinatorial background. Figure 3(a) shows the resulting mass difference ($\Delta M = M_{J\gamma} - M_J$). Since the production of χ_{c0} and χ_{c2} is expected to be suppressed in b decays, we interpret the enhancement of events as coming solely from χ_{c1} . The background comes mainly from J mesons paired with photons produced either in the b decay chain or in the fragmentation process. This background is simulated using JETSET Monte Carlo b flavor events, requiring the decay chain $b \rightarrow J + X$ followed by $J \rightarrow \mu^+ \mu^-$ and then reconstructing the mass difference ΔM shown in Figure 3(b). The background from photons paired with dimuons from cascade decays has been determined and has the same shape as the dominant background. The acceptance calculation is based on Monte Carlo events with the decay chain $b \rightarrow \chi_{c1} + X$ followed by $\chi_{c1} \rightarrow J + \gamma$ followed by $J \rightarrow \mu^+ \mu^-$. The acceptance for this process is calculated to be $\varepsilon_{\chi_{c1}} = 0.10 \pm 0.01$ [13] including the acceptance of the J. Note that the acceptance calculation would not change if χ_{c2} were produced in b decays and that χ_{c0} has a too small a branching ratio into $J + \gamma$ to be detected with the present statistics.

6 Determination of $\text{Br}(\mathbf{Z} \rightarrow \chi_{c1} + \mathbf{X})$

We fit the invariant mass distribution shown in Figure 3(a) with a Gaussian for the signal and a background shape as shown in Figure 3(b). The normalization of the background is left free in the fit. We find 19 ± 7 χ_c candidates with a mass difference of 445 ± 20 MeV and a width of 54 ± 26 MeV. This is compatible with the $(\chi_{c1} - \mathbf{J})$ mass difference 421 ± 3 MeV and width 31 ± 2 MeV for the Monte Carlo events.

Folding in the geometrical and kinematical acceptances, we find

$$\text{Br}(\mathbf{Z} \rightarrow \chi_{c1} + \mathbf{X}) = (7.5 \pm 2.9 \text{ (stat.)} \pm 0.6 \text{ (sys.)}) \times 10^{-3}.$$

The sources of systematic error are the fitting method, the errors on the branching ratios $\text{Br}(\mathbf{J} \rightarrow \mu^+ \mu^-)$ and $\text{Br}(\chi_{c1} \rightarrow \mathbf{J} \gamma)$ and the error on the efficiency. The dominant error is from the fitting method, and was determined by changing the fit window, as well as the background shape.

If we assume that all the χ_{c1} are produced in b decays, we obtain

$$\text{Br}(\mathbf{b} \rightarrow \chi_{c1} + \mathbf{X}) = (2.4 \pm 0.9 \text{ (stat.)} \pm 0.2 \text{ (sys.)}) \times 10^{-2}.$$

The measured branching ratio for $\mathbf{b} \rightarrow \chi_{c1} + \mathbf{X}$ is in agreement with the value obtained by ARGUS [5] $(1.23 \pm 0.41 \pm 0.29) \times 10^{-2}$, where we have recalculated their value using the MARK III $\mathbf{J} \rightarrow \mu^+ \mu^-$ branching ratio measurement.

We also compute the ratio

$$\frac{\text{Br}(\mathbf{b} \rightarrow \chi_{c1} + \mathbf{X})}{\text{Br}(\mathbf{b} \rightarrow \mathbf{J} + \mathbf{X})} = 1.92 \pm 0.82.$$

This ratio which is less sensitive to the color-suppression effects, is higher than the theoretical model expectation value 0.27 [1,2]. This higher value implies that a non-negligible fraction of \mathbf{J} mesons produced in b decay come from the decay of χ_c mesons. This ratio has been computed using the $\text{Br}(\mathbf{b} \rightarrow \mathbf{J} + \mathbf{X})$ from the $\mu^+ \mu^-$ channel as some systematic errors cancel.

This result has been obtained assuming that only χ_{c1} are produced in b decays. As the branching ratio of χ_{c0} and χ_{c2} to $\mathbf{J} + \gamma$ is smaller than that of χ_{c1} , any admixture of χ_{c0} or χ_{c2} , as for example, in the color octet model [15], will only increase the inferred ratio of χ_c to \mathbf{J} .

7 Conclusion

We have observed χ_c production at LEP. Using the decay channel $\chi_c \rightarrow \mathbf{J} + \gamma$, and attributing all events to χ_{c1} , we have determined the branching ratio $\text{Br}(\mathbf{Z} \rightarrow \chi_{c1} + \mathbf{X}) = (7.5 \pm 2.9 \text{ (stat.)} \pm 0.6 \text{ (sys.)}) \times 10^{-3}$. Assuming that only χ_{c1} are produced in b decays, we obtain a branching ratio $\text{Br}(\mathbf{b} \rightarrow \chi_{c1} + \mathbf{X}) = (2.4 \pm 0.9 \text{ (stat.)} \pm 0.2 \text{ (sys.)}) \times 10^{-2}$.

8 Acknowledgments

We wish to express our gratitude to the CERN accelerator divisions for the excellent performance of the LEP machine. We acknowledge the contributions of all the engineers and technicians who have participated in the construction and maintenance of this experiment. We would like to thank Prof. J. H. Kühn and Prof. R. Rückl for very useful discussions.

References

- [1] J. H. Kühn, S. Nussinov and R. Rückl, *Z. Phys.* **C 5** (1980) 117.
- [2] J. H. Kühn and R. Rückl, *Phys. Lett.* **B 135** (1984) 477.
- [3] P. H. Cox *et al.*, *Phys. Rev.* **D 32** (1985) 1157.
- [4] H. Fritzsch, *Phys. Lett.* **B 86** (1979) 164, 343.
- [5] ARGUS Collaboration, H. Albrecht *et al.*, *Phys. Lett.* **B 277** (1992) 209.
- [6] L3 Collaboration, B. Adeva *et al.*, *Nucl. Inst. and Meth.* **A289** (1990) 35.
- [7] L3 Collaboration, B. Adeva *et al.*, *Phys. Lett.* **B 252** (1990) 703
- [8] L3 Collaboration, B. Adeva *et al.*, *Phys. Lett.* **B 288** (1992) 412.
- [9] L3 Collaboration, B. Adeva *et al.*, *Phys. Lett.* **B 307** (1993) 237.
- [10] L3 Collaboration, B. Adeva *et al.*, *Phys. Lett.* **B 259** (1991) 199.
- [11] T. Sjöstrand and M. Bengtsson, *Comput. Phys. Commun.* **43** (1987) 367;
T. Sjöstrand in “Z Physics at LEP”, CERN Report CERN-89-08, Vol. III, p. 143.
For the 1990 data we used JETSET 7.2 and for the 1991 and 1992 data we used JETSET 7.3.
- [12] L3 Collaboration, B. Adeva *et al.*, *Phys. Lett.* **B 307** (1993) 451.
- [13] M. Wadhwa, Etude de la production de J/ψ et de χ_c dans les désintégrations du Z avec le détecteur L3 à LEP, Ph.D. thesis, L’Université de Savoie (France 1993).
- [14] MARK-III Collaboration, D. Coffman *et al.*, *Phys. Rev. Lett.* **68** (1992) 282.
- [15] G. T. Bodwin *et al.*, *Phys. Rev.* **D 46** (1992) 3703.

The L3 Collaboration:

O. Adriani,¹⁵ M. Aguilar-Benitez,²⁴ S. Ahlen,⁹ J. Alcaraz,¹⁶ A. Aloisio,²⁷ G. Alverson,¹⁰ M.G. Alviggi,²⁷ G. Ambrosi,³² Q. An,¹⁷ H. Anderhub,⁴⁶ A.L. Anderson,¹⁴ V.P. Andreev,³⁶ T. Angelescu,¹¹ L. Antonov,⁴⁰ D. Antreasyan,⁷ P. Arce,²⁴ A. Arefev,²⁶ A. Atamanchuk,³⁶ T. Azemoon,³ T. Aziz,⁸ P.V.K.S. Baba,¹⁷ P. Bagnaia,³⁵ J.A. Bakken,³⁴ R.C. Ball,³ S. Banerjee,⁸ J. Bao,⁵ R. Barillère,¹⁶ L. Barone,³⁵ A. Baschirotto,²⁵ R. Battiston,³² A. Bay,¹⁸ F. Becattini,¹⁵ J. Bechtluft,¹ R. Becker,¹ U. Becker,^{14,46} F. Behner,⁴⁶ J. Behrens,⁴⁶ Gy.L. Bencze,¹² J. Berdugo,²⁴ P. Berges,¹⁴ B. Bertucci,³² B.L. Betev,^{40,46} M. Biasini,³² A. Biland,⁴⁶ G.M. Bilei,³² R. Bizzarri,³⁵ J.J. Blaising,⁴ G.J. Bobbink,^{16,2} R. Bock,¹ A. Böhm,¹ B. Borgia,³⁵ M. Bosetti,²⁵ D. Bourilkov,²⁹ M. Bourquin,¹⁸ D. Boutigny,¹⁶ B. Bouwens,² E. Brambilla,²⁷ J.G. Branson,³⁷ I.C. Brock,³³ M. Brooks,²² A. Bujak,⁴³ J.D. Burger,¹⁴ W.J. Burger,¹⁸ J. Busenitz,⁴² A. Buytenhuijs,²⁹ X.D. Cai,¹⁷ M. Capell,¹⁴ M. Caria,³² G. Carlino,²⁷ A.M. Cartacci,¹⁵ R. Castello,²⁵ M. Cerrada,²⁴ F. Cesaroni,³⁵ Y.H. Chang,¹⁴ U.K. Chaturvedi,¹⁷ M. Chemarin,²³ A. Chen,⁴⁸ C. Chen,⁶ G. Chen,⁶ G.M. Chen,⁶ H.F. Chen,¹⁹ H.S. Chen,⁶ M. Chen,¹⁴ W.Y. Chen,⁴⁸ G. Chiefari,²⁷ C.Y. Chien,⁵ M.T. Choi,⁴¹ S. Chung,¹⁴ C. Cividini,¹⁵ I. Clare,¹⁴ R. Clare,¹⁴ T.E. Coan,²² H.O. Cohn,³⁰ G. Coignet,⁴ N. Colino,¹⁶ A. Contin,⁷ S. Costantini,³⁵ F. Cotorobai,¹¹ X.T. Cui,¹⁷ X.Y. Cui,¹⁷ T.S. Dai,¹⁴ R.D. Alessandro,¹⁵ R. de Asmundis,²⁷ A. Degre,⁴ K. Deiters,⁴⁴ E. Dénes,¹² P. Denes,³⁴ F. DeNotaristefani,³⁵ M. Dhina,⁴⁶ D. DiBitonto,⁴² M. Diemoz,³⁵ H.R. Dimitrov,⁴⁰ C. Dionisi,³⁵ M. Dittmar,⁴⁶ L. Djambazov,⁴⁶ M.T. Dova,¹⁷ E. Drago,²⁷ D. Duchesneau,¹⁸ P. Duinker,² I. Duran,³⁸ S. Easo,³² H. El Mamouni,²³ A. Engler,³³ F.J. Eppling,¹⁴ F.C. Ern e,² P. Extermann,¹⁸ R. Fabbretti,⁴⁴ M. Fabre,⁴⁴ S. Falciano,³⁵ S.J. Fan,³⁹ O. Fackler,²¹ J. Fay,²³ M. Felcini,¹⁶ T. Ferguson,³³ D. Fernandez,²⁴ G. Fernandez,²⁴ F. Ferroni,³⁵ H. Fesefeldt,¹ E. Fiandrini,³² J.H. Field,¹⁸ F. Filthaut,²⁹ P.H. Fisher,⁵ G. Forconi,¹⁸ L. Fredj,¹⁸ K. Freudenreich,⁴⁶ W. Friebel,⁴⁵ M. Fukushima,¹⁴ M. Gaillard,²⁶ Yu. Galaktionov,^{26,14} E. Gallo,¹⁵ S.N. Ganguli,^{16,8} P. Garcia-Abia,²⁴ D. Gele,²³ S. Gentile,³⁵ N. Gheordanescu,¹¹ S. Giagu,³⁵ S. Goldfarb,²⁰ Z.F. Gong,¹⁹ E. Gonzalez,²⁴ A. Gougas,⁵ D. Goujon,¹⁸ G. Gratta,³¹ M. Gruenewald,¹⁶ C. Gu,¹⁷ M. Guanzirolı,¹⁷ J.K. Guo,³⁹ V.K. Gupta,³⁴ A. Gurtu,⁸ H.R. Gustafson,³ L.J. Gutay,⁴³ K. Hangarter,¹ B. Hartmann,¹ A. Hasan,¹⁷ D. Hauschildt,² C.F. He,³⁹ J.T. He,⁶ T. Hebbeker,¹⁶ M. Hebert,³⁷ A. Herv e,¹⁶ K. Hilgers,¹ H. Hofer,⁴⁶ H. Hoorani,¹⁸ G. Hu,¹⁷ G.Q. Hu,³⁹ B. Ille,²³ M.M. Ilyas,¹⁷ V. Innocente,¹⁶ H. Janssen,¹⁶ S. Jezequel,⁴ B.N. Jin,⁶ L.W. Jones,³ I. Josa-Mutuberria,¹⁶ A. Kasser,²⁰ R.A. Khan,¹⁷ Yu. Kamyshkov,³⁰ P. Kapinos,^{36,45} J.S. Kapustinsky,²² Y. Karyotakis,¹⁶ M. Kaur,¹⁷ S. Khokhar,¹⁷ M.N. Kienzle-Focacci,¹⁸ J.K. Kim,⁴¹ S.C. Kim,⁴¹ Y.G. Kim,⁴¹ W.W. Kinnison,²² A. Kirkby,³¹ D. Kirkby,³¹ S. Kirsch,⁴⁵ W. Kittel,²⁹ A. Klimentov,^{14,26} R. Kl ockner,¹ A.C. K onig,²⁹ E. Koffeman,² O. Kornadt,¹ V. Koutsenko,^{14,26} A. Koulbardi,³⁶ R.W. Kraemer,³³ T. Kramer,¹⁴ V.R. Krastev,^{40,32} W. Krenz,¹ A. Krivshich,³⁶ H. Kuijten,²⁹ K.S. Kumar,¹³ A. Kunin,^{14,26} G. Landi,¹⁵ D. Lanske,¹ S. Lanzano,²⁷ A. Lebedev,¹⁴ P. Lebrun,²³ P. Lecomte,⁴⁶ P. Lecoq,¹⁶ P. Le Coultre,⁴⁶ D.M. Lee,²² J.S. Lee,⁴¹ K.Y. Lee,⁴¹ I. Leedom,¹⁰ C. Leggett,³ J.M. Le Goff,¹⁶ R. Leiste,⁴⁵ M. Lenti,¹⁵ E. Leonardi,³⁵ C. Li,^{19,17} H.T. Li,⁶ P.J. Li,³⁹ J.Y. Liao,³⁹ W.T. Lin,⁴⁸ Z.Y. Lin,¹⁹ F.L. Linde,² B. Lindemann,¹ L. Lista,²⁷ Y. Liu,¹⁷ W. Lohmann,⁴⁵ E. Longo,³⁵ Y.S. Lu,⁶ J.M. Lubbers,¹⁶ K. L ubelsmeyer,¹ C. Luci,³⁵ D. Luckey,^{7,14} L. Ludovici,³⁵ L. Luminari,³⁵ W. Lustermann,⁴⁵ J.M. Ma,¹⁹ M. MacDermott,⁴⁶ R. Malik,¹⁷ A. Malinin,²⁶ C. Ma a,²⁴ M. Maolinbay,⁴⁶ P. Marchesini,⁴⁶ F. Marion,⁴ A. Marin,⁹ J.P. Martin,²³ L. Martinez-Laso,²⁴ F. Marzano,³⁵ G.G.G. Massaro,² K. Mazumdar,¹⁸ P. McBride,¹³ T. McMahan,⁴³ D. McNally,⁴⁶ M. Merk,³³ L. Merola,²⁷ M. Meschini,¹⁵ W.J. Metzger,²⁹ Y. Mi,²⁰ A. Mihul,¹ G.B. Mills,²² Y. Mir,¹⁷ G. Mirabelli,³⁵ J. Mnich,¹ M. M oller,¹ B. Monteleoni,¹⁵ R. Morand,⁴ S. Morganti,³⁵ N.E. Moulai,¹⁷ R. Mount,³¹ S. M uller,¹ A. Nadochay,³⁶ E. Nagy,¹² M. Napolitano,²⁷ F. Nessi-Tedaldi,⁴⁶ H. Newman,³¹ C. Neyer,⁴⁶ M.A. Niaz,¹⁷ A. Nippe,¹ H. Nowak,⁴⁵ G. Organtini,³⁵ D. Pandoulas,¹ S. Paoletti,³⁵ P. Paolucci,²⁷ G. Pascale,³⁵ G. Passaleva,^{15,32} S. Patricelli,²⁷ T. Paul,⁵ M. Pauluzzi,³² C. Paus,¹ F. Pauss,⁴⁶ Y.J. Pei,¹ S. Pensotti,²⁵ D. Perret-Gallix,⁴ J. Perrier,¹⁸ A. Pevsner,⁵ D. Piccolo,²⁷ M. Pieri,¹⁶ P.A. Pirou e,³⁴ F. Plasil,³⁰ V. Plyaskin,²⁶ M. Pohl,⁴⁶ V. Pojidaev,^{26,15} H. Postema,¹⁴ Z.D. Qi,³⁹ J.M. Qian,³ K.N. Qureshi,¹⁷ R. Raghavan,⁸ G. Rahal-Callot,⁴⁶ P.G. Rancoita,²⁵ M. Rattaggi,²⁵ G. Raven,² P. Razi, ²⁸ K. Read,³⁰ D. Ren,⁴⁶ Z. Ren,¹⁷ M. Rescigno,³⁵ S. Reucroft,¹⁰ A. Ricker,¹ S. Riemann,⁴⁵ B.C. Riemers,⁴³ K. Riles,³ O. Rind,³ H.A. Rizvi,¹⁷ S. Ro,⁴¹ F.J. Rodriguez,²⁴ B.P. Roe,³ M. R ohner,¹ L. Romero,²⁴ S. Rosier-Lees,⁴ R. Rosmalen,²⁹ Ph. Rosselet,²⁰ W. van Rossum,² S. Roth,¹ A. Rubbia,¹⁴ J.A. Rubio,¹⁶ H. Rykaczewski,⁴⁶ M. Sachwitz,⁴⁵ J. Salicio,¹⁶ J.M. Salicio,²⁴ G.S. Sanders,²² A. Santocchia,³² M.S. Sarakinos,¹⁴ G. Sartorelli,^{7,17} M. Sassowsky,¹ G. Sauvage,⁴ V. Schegelsky,³⁶ D. Schmitz,¹ P. Schmitz,¹ M. Schneegans,⁴ H. Schopper,⁴⁷ D.J. Schotanus,²⁹ S. Shotkin,¹⁴ H.J. Schreiber,⁴⁵ J. Shukla,³³ R. Schulte,¹ S. Schulte,¹ K. Schultze,¹ J. Schwenke,¹ G. Schwering,¹ C. Sciacca,²⁷ I. Scott,¹³ R. Sehgal,¹⁷ P.G. Seiler,⁴⁴ J.C. Sens,^{16,2} L. Servoli,³² I. Sheer,³⁷ D.Z. Shen,³⁹ S. Shevchenko,³¹ X.R. Shi,³¹ E. Shumilov,²⁶ V. Shoutko,²⁶ D. Son,⁴¹ A. Sopczak,¹⁶ V. Soulimov,²⁷ C. Spartiotsis,⁵ T. Spickermann,¹ P. Spillantini,¹⁵ R. Starosta,¹ M. Steuer,^{7,14} D.P. Stickland,³⁴ F. Sticozzi,¹⁴ H. Stone,³⁴ K. Strauch,¹³ B.C. Stringfellow,⁴³ K. Sudhakar,⁸ G. Sultanov,¹⁷ L.Z. Sun,^{19,17} G.F. Susinno,¹⁸ H. Suter,⁴⁶ J.D. Swain,¹⁷ A.A. Syed,²⁹ X.W. Tang,⁶ L. Taylor,¹⁰ G. Terzi,²⁵ Samuel C.C. Ting,¹⁴ S.M. Ting,¹⁴ M. Tonutti,¹ S.C. Tonwar,⁸ J. T oth,¹² A. Tsaregorodtsev,³⁶ G. Tsipolitis,³³ C. Tully,³⁴ K.L. Tung,⁶ J. Ulbricht,⁴⁶ L. Urb an,¹² U. Uwer,¹ E. Valente,³⁵ R.T. Van de Walle,²⁹ I. Vetlitsky,²⁶ G. Viertel,⁴⁶ P. Vikas,¹⁷ U. Vikas,¹⁷ M. Vivargent,⁴ H. Vogel,³³ H. Vogt,⁴⁵ I. Vorobiev,^{13,26} A.A. Vorobyov,³⁶ L. Vuilleumier,²⁰ M. Wadhwa,⁴ W. Wallraff,¹ C. Wang,¹⁴ C.R. Wang,¹⁹ X.L. Wang,¹⁹ Y.F. Wang,¹⁴ Z.M. Wang,^{17,19} C. Warner,¹ A. Weber,¹ J. Weber,⁴⁶ R. Weill,²⁰ T.J. Wenaus,²¹ J. Wenninger,¹⁸ M. White,¹⁴ C. Willmott,²⁴ F. Wittgenstein,¹⁶ D. Wright,³⁴ S.X. Wu,¹⁷ S. Wynhoff,¹ B. Wyslouh,¹⁴ Y.Y. Xie,³⁹ J.G. Xu,⁶ Z.Z. Xu,¹⁹ Z.L. Xue,³⁹ D.S. Yan,³⁹ B.Z. Yang,¹⁹ C.G. Yang,⁶ G. Yang,¹⁷ C.H. Ye,¹⁷ J.B. Ye,¹⁹ Q. Ye,¹⁷ S.C. Yeh,⁴⁸ Z.W. Yin,³⁹ J.M. You,¹⁷ N. Yunus,¹⁷ M. Yzerman,² C. Zaccardelli,³¹ N. Zaitsev,²⁷ P. Zemp,⁴⁶ M. Zeng,¹⁷ Y. Zeng,¹ D.H. Zhang,² Z.P. Zhang,^{19,17} B. Zhou,⁹ G.J. Zhou,⁶ J.F. Zhou,¹ R.Y. Zhu,³¹ A. Zichichi,^{7,16,17} B.C.C. van der Zwaan,²

-
- 1 I. Physikalisches Institut, RWTH, W-5100 Aachen, FRG[§]
 - III. Physikalisches Institut, RWTH, W-5100 Aachen, FRG[§]
 - 2 National Institute for High Energy Physics, NIKHEF, NL-1009 DB Amsterdam, The Netherlands
 - 3 University of Michigan, Ann Arbor, MI 48109, USA
 - 4 Laboratoire d'Annecy-le-Vieux de Physique des Particules, LAPP,IN2P3-CNRS, BP 110, F-74941 Annecy-le-Vieux CEDEX, France
 - 5 Johns Hopkins University, Baltimore, MD 21218, USA
 - 6 Institute of High Energy Physics, IHEP, 100039 Beijing, China
 - 7 INFN-Sezione di Bologna, I-40126 Bologna, Italy
 - 8 Tata Institute of Fundamental Research, Bombay 400 005, India
 - 9 Boston University, Boston, MA 02215, USA
 - 10 Northeastern University, Boston, MA 02115, USA
 - 11 Institute of Atomic Physics and University of Bucharest, R-76900 Bucharest, Romania
 - 12 Central Research Institute for Physics of the Hungarian Academy of Sciences, H-1525 Budapest 114, Hungary[‡]
 - 13 Harvard University, Cambridge, MA 02139, USA
 - 14 Massachusetts Institute of Technology, Cambridge, MA 02139, USA
 - 15 INFN Sezione di Firenze and University of Florence, I-50125 Florence, Italy
 - 16 European Laboratory for Particle Physics, CERN, CH-1211 Geneva 23, Switzerland
 - 17 World Laboratory, FBLJA Project, CH-1211 Geneva 23, Switzerland
 - 18 University of Geneva, CH-1211 Geneva 4, Switzerland
 - 19 Chinese University of Science and Technology, USTC, Hefei, Anhui 230 029, China
 - 20 University of Lausanne, CH-1015 Lausanne, Switzerland
 - 21 Lawrence Livermore National Laboratory, Livermore, CA 94550, USA
 - 22 Los Alamos National Laboratory, Los Alamos, NM 87544, USA
 - 23 Institut de Physique Nucléaire de Lyon, IN2P3-CNRS, Université Claude Bernard, F-69622 Villeurbanne Cedex, France
 - 24 Centro de Investigaciones Energeticas, Medioambientales y Tecnologicas, CIEMAT, E-28040 Madrid, Spain
 - 25 INFN-Sezione di Milano, I-20133 Milan, Italy
 - 26 Institute of Theoretical and Experimental Physics, ITEP, Moscow, Russia
 - 27 INFN-Sezione di Napoli and University of Naples, I-80125 Naples, Italy
 - 28 Department of Natural Sciences, University of Cyprus, Nicosia, Cyprus
 - 29 University of Nymegen and NIKHEF, NL-6525 ED Nymegen, The Netherlands
 - 30 Oak Ridge National Laboratory, Oak Ridge, TN 37831, USA
 - 31 California Institute of Technology, Pasadena, CA 91125, USA
 - 32 INFN-Sezione di Perugia and Università Degli Studi di Perugia, I-06100 Perugia, Italy
 - 33 Carnegie Mellon University, Pittsburgh, PA 15213, USA
 - 34 Princeton University, Princeton, NJ 08544, USA
 - 35 INFN-Sezione di Roma and University of Rome, "La Sapienza", I-00185 Rome, Italy
 - 36 Nuclear Physics Institute, St. Petersburg, Russia
 - 37 University of California, San Diego, CA 92093, USA
 - 38 Dept. de Fisica de Particulas Elementales, Univ. de Santiago, E-15706 Santiago de Compostela, Spain
 - 39 Shanghai Institute of Ceramics, SIC, Shanghai, China
 - 40 Bulgarian Academy of Sciences, Institute of Mechatronics, BU-1113 Sofia, Bulgaria
 - 41 Center for High Energy Physics, Korea Advanced Inst. of Sciences and Technology, 305-701 Taejon, Republic of Korea
 - 42 University of Alabama, Tuscaloosa, AL 35486, USA
 - 43 Purdue University, West Lafayette, IN 47907, USA
 - 44 Paul Scherrer Institut, PSI, CH-5232 Villigen, Switzerland
 - 45 DESY-Institut für Hochenergiephysik, O-1615 Zeuthen, FRG
 - 46 Eidgenössische Technische Hochschule, ETH Zürich, CH-8093 Zürich, Switzerland
 - 47 University of Hamburg, W-2000 Hamburg, FRG
 - 48 High Energy Physics Group, Taiwan, China
- § Supported by the German Bundesministerium für Forschung und Technologie
‡ Supported by the Hungarian OTKA fund under contract number 2970.

Figure Captions

Figure 1: Diagram for $b(\bar{b}) \rightarrow [c\bar{c}] + X$.

Figure 2: The invariant mass distributions of $\mu^+\mu^-$ and e^+e^- pairs.

Figure 3: The ΔM Distribution for (a) Data and (b) Monte Carlo background shape. The peak in the data is interpreted as a χ_c signal.

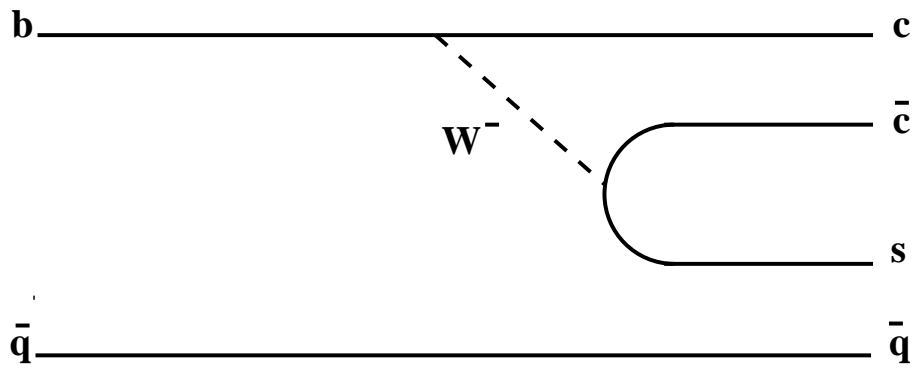


Figure 1:

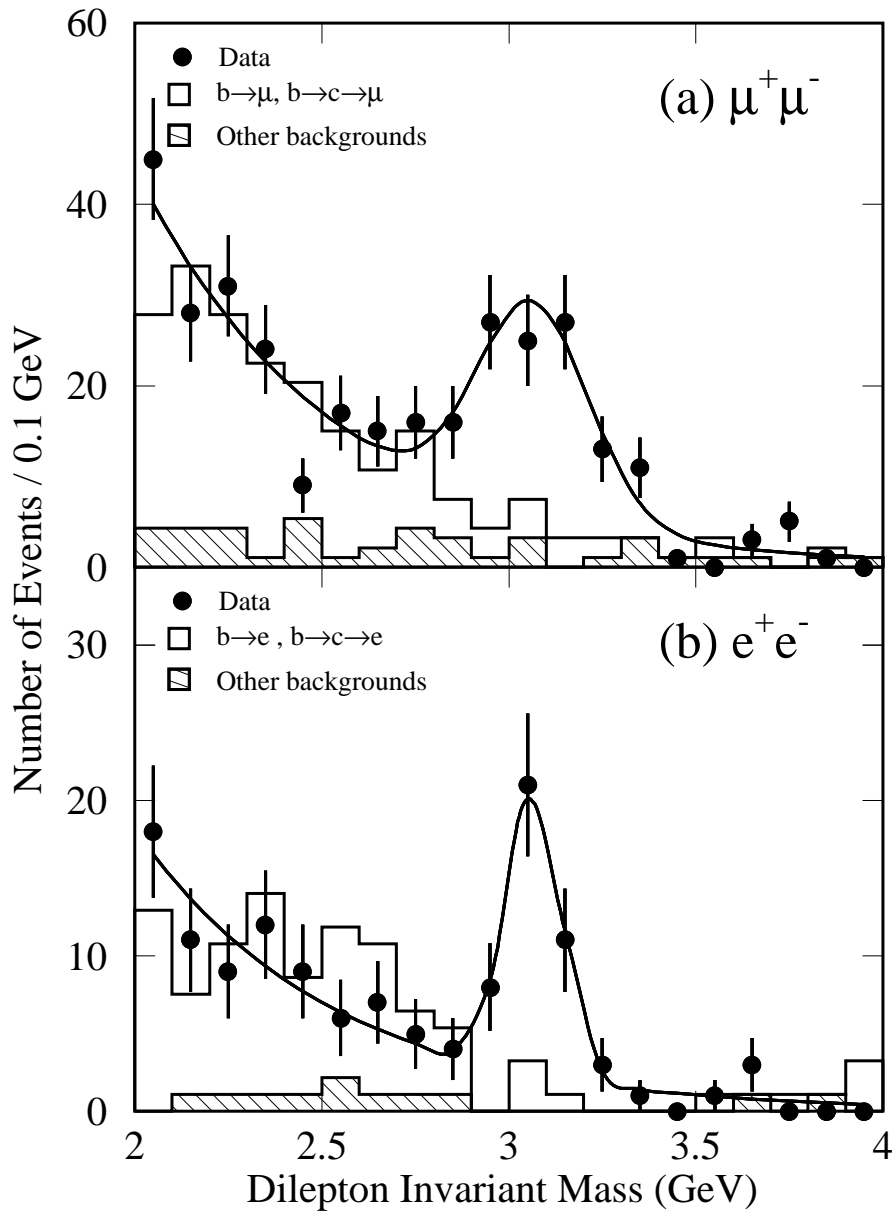


Figure 2:

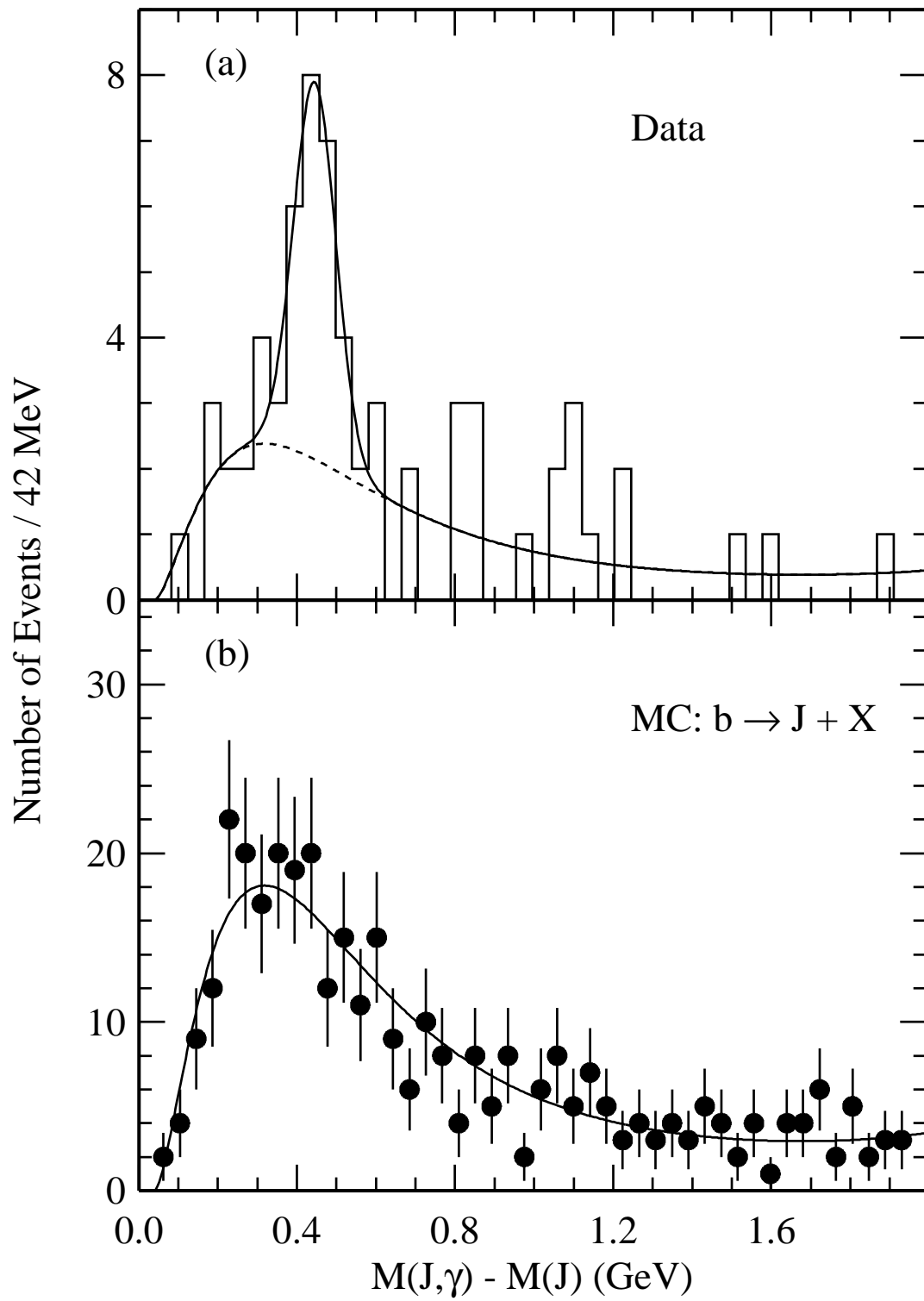


Figure 3: